FULL PAPER

Dalton
www.rsc.org/dalton

Synthetic, spectroscopic and olefin oligomerisation studies on nickel and palladium complexes containing ferrocene substituted nitrogen donor ligands

Vernon C. Gibson,* Catherine M. Halliwell, Nicholas J. Long,* Philip J. Oxford, Andrew M. Smith, Andrew J. P. White and David J. Williams

Imperial College of Science, Technology and Medicine, Exhibition Road, South Kensington, London, UK SW7 2AY. E-mail: n.long@ic.ac.uk. E-mail: v.gibson@ic.ac.uk; Fax: 020 7594 5804; Tel: 020 7594 5781

Received 24th October 2002, Accepted 3rd January 2003
First published as an Advance Article on the web 30th January 2003

A series of new pyridyl- and quinolyl-N-substituted ferrocenyl and ferrocenediyl ligands have been conveniently synthesised and characterised and their coordination chemistry probed by reaction with a range of nickel and palladium reagents. The bidentate, chelating nature of each arm is demonstrated, especially using X-ray crystallography, though subtle changes in the steric bulk around the ligand enforces other bonding modes. Electrochemical studies show the expected shift of the Fe^{II}/Fe^{III} redox couple on coordination of the metal centre(s) to the ligands, and polymerisation studies indicate that the nickel-based complexes act as very efficient pre-catalysts for the formation of short chain oligomers.

Introduction

In coordination chemistry, the ferrocenyl moiety has played a significant role as a backbone or a substituent in ancillary ligands due to (i) the specific and unique geometries that the ferrocene provides and (ii) its electronic (redox) properties, whereby the possibility of switching the redox state of the ferrocene backbone gives access to potential control of reactivity at a metal centre. Redox active ligands have been increasingly utilised in order to perturb the electronic properties and stoichiometric reactivity of the transition metals to which they are bound.[1,2] As such, these species offer exciting potential within homogeneous transition metal catalysis, since the oxidation of a redox-active substituent induces a higher electrophilicity and therefore a change in reactivity of a catalytically-active transition metal centre.

The gamut of ligands formed *via* substitution of ferrocenes by various donor heteroatoms have found wide application.[3,4] Although substituted ferrocenyl amines are known,[5] the formation of N-substituted ferrocenyl and ferrocenediyl species has been hampered by the lack of good synthetic methods. However, in recent years more efficient routes to the synthesis of the primary amine, $FcNH_2$ (Fc = ferrocenyl)[6] and the diamine, 1,1′-diaminoferrocene[7] have opened up the area. Indeed, the titanium and zirconium complexes of these and related ligands[8–10] have recently been highlighted.[11] We have been interested in forming new sterically hindered and redox-active nitrogen-substituted ferrocene ligands to investigate their coordination chemistry and application in catalysis, particularly olefin polymerisation.

In recent years, complexes of the late transition metals have had an important role to play as olefin polymerisation pre-catalysts.[12,13] Nickel and palladium complexes of diimine, unsymmetrical imino pyridine, and dipyridylamine ligands have been reported and examined for their catalytic activities.[14] To probe this further, a range of new mono- and di-N-substituted ferrocene ligands and their nickel and palladium complexes have been synthesised and characterised and are reported here, along with preliminary investigations into their activity as pre-catalysts for olefin polymerisation.

Results and discussion

The ferrocenediyl ligands **1A–C** were synthesised in excellent yields *via* the condensation reaction of 1,1′-diaminoferrocene with the appropriate heterocyclic aldehyde (Scheme 1). Slightly more forcing conditions were required for the formation of the ferrocenyl ligands **2A–C**, with stirring of dichloromethane solutions of ferrocenylamine and the heterocyclic aldehyde at 40 °C. Again, good yields were obtained and the red/burgundy coloured solids were characterised by microanalysis, ^1H and $^{13}C\{^1H\}$ NMR spectroscopy and mass spectrometry.

The X-ray structures of two amino-functionalised ligands **1A** and **1C** have been determined and are shown to have very similar conformations, with their pairs of imino linkages and their pyridyl and quinoline ring systems in parallel alignments (Figs. 1 and 2) and at interacting π–π stacking separations. In both structures the molecular symmetry departs from C_s, the planes of the nitrogen-containing ring systems being tilted with respect to their adjacent C_5H_4 rings. In **1A** these inclinations differ with the N(13)-containing pyridyl ring inclined by *ca.* 10° whereas its N(20)-containing counterpart is inclined by *ca.* 19°, the two pyridyl rings being mutually inclined by *ca.* 11°. In **1C** the quinoline rings are mutually inclined by only *ca.* 3°, though each is inclined by *ca.* 22° to its associated C_5H_4 ring. The ferrocenediyl units in both structures have essentially eclipsed geometries with both stagger and interplanar angles of less than 3°. Despite the relatively small departures from coplanarity of the C_5H_4 and pyridine/quinoline ring systems there is no significant delocalisation of the central C=N double bonds [C=N in the

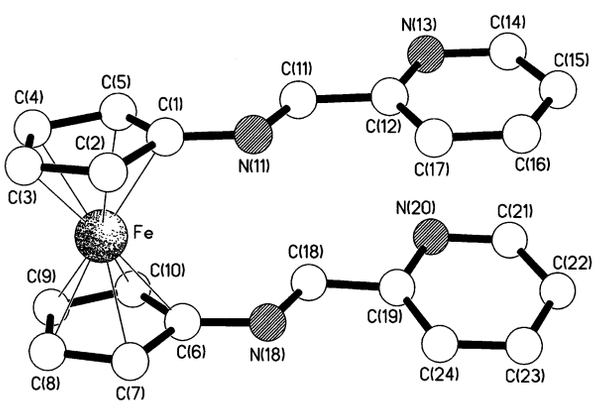

Fig. 1 The molecular structure of **1A**. Selected bond lengths (Å): N(11)–C(11) 1.269(4), N(18)–C(18) 1.268(4). The centroid · · · centroid separations between the two imine bonds and the two pyridyl rings are 3.41 and 3.70 Å, respectively.

DOI: 10.1039/b210463f

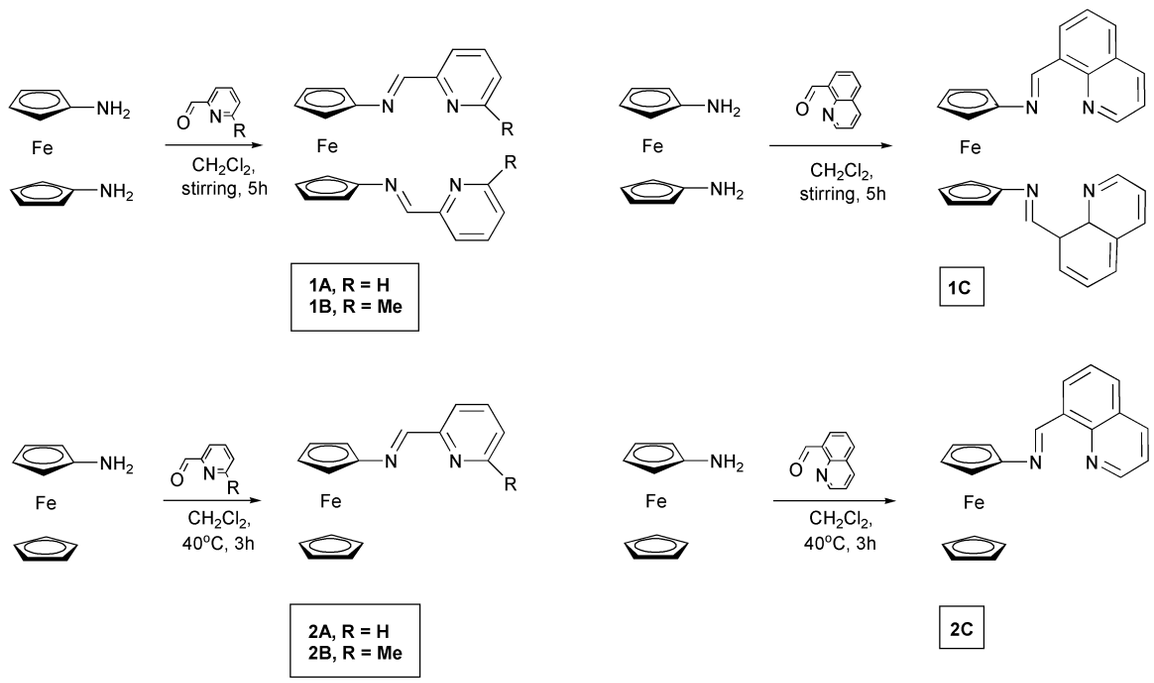

Scheme 1 Formation of ligands **1A**–**2C**.

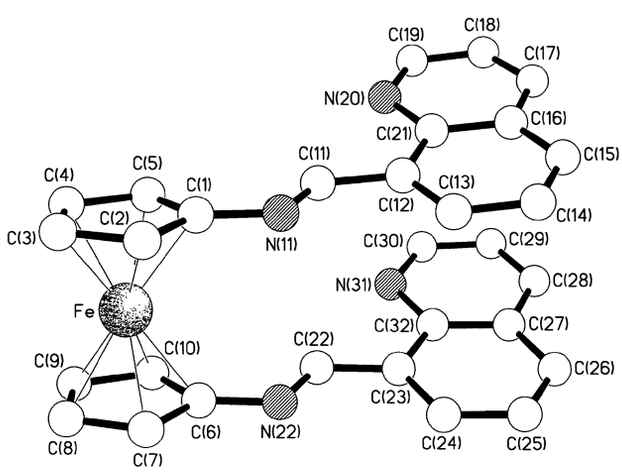

Fig. 2 One of the pair of crystallographically independent molecules present in the structure of **1C** (the conformation of the second molecule is essentially identical). Selected bond lengths (Å) (values for the second independent molecule in square parentheses): N(11)–C(11) 1.268(6) [1.259(7)], N(22)–C(22) 1.269(7) [1.269(7)]. The centroid ··· centroid separations between the two imine bonds and the two quinoline rings are 3.40 [3.47] and 3.75 [3.77] Å, respectively.

range 1.259(7)–1.269(7) Å across both structures]. A feature of both structures is the *anti* geometry of the imino and ring nitrogen atoms, indicating that appreciable conformational change is required for chelation to a second metal centre. In **1A** there is an intermolecular C–H ··· π interaction between C(3)–H in one molecule and the C(6)–C(10) cyclopentadienyl ring of another (H ··· π 2.87 Å, C–H ··· π 148°), and an orthogonal C–H ··· N(pπ) approach from C(8)–H in one molecule to N(18) in another (H ··· N 2.55 Å, C–H ··· N 165°). There are no intermolecular packing interactions of note in the structure of **1C**.

The ligands were then treated with nickel and palladium reagents to illustrate the bidentate, chelating nature of each ligand 'arm' (Scheme 2). For example, dichloromethane solutions of $NiBr_2$·dme (dme = 1,2-dimethoxyethane) and the various ligands were mixed and heated at reflux for 18–20 h, after which an indigo-coloured precipitate formed which was washed and dried '*in vacuo*'. The air- and moisture-sensitive nickel(II) complexes **3A**–**C**, **4A**–**C** (Scheme 2) were formed in reasonable yields and characterised by microanalysis and FAB mass spectrometry.

The palladium complexes **5A**–**D**, **6A**–**D**, were formed in a similar fashion, with dichloromethane solutions of the ligands and $(COD)PdCl_2$ or (COD)PdCl(Me) mixed together and stirred for 18–20 h. The reactions proceeded smoothly and any unreacted starting material was washed off and/or the crude product was recrystallised from dichloromethane–hexane (1 : 1) solutions. Good yields were obtained and the new products characterised by microanalysis, ^{1}H NMR (poor solubility precluded ^{13}C-{^{1}H} NMR studies) and mass spectrometry.

Single crystal X-ray analysis showed that complex **6B** had the desired structure with the palladium centre chelated by the imino and pyridyl nitrogen atoms (Fig. 3, Table 1). The crystals contain two independent molecules (A and B) with noticeably different geometries. Both have the methyl substituent *trans* to the imino nitrogen and have essentially the same *cis* angles at the palladium centre (in the ranges 78.6(2)–93.0(3)° and 79.1(2)–91.8(3)° for molecules A and B, respectively). However, in one molecule (A) the chelate ring and its associated pyridyl ring are coplanar to within 0.06 Å with the chlorine atom lying 0.34 Å out of plane in the direction of the unsubstituted cyclopentadienyl ring, whereas in molecule B the chelate and pyridyl

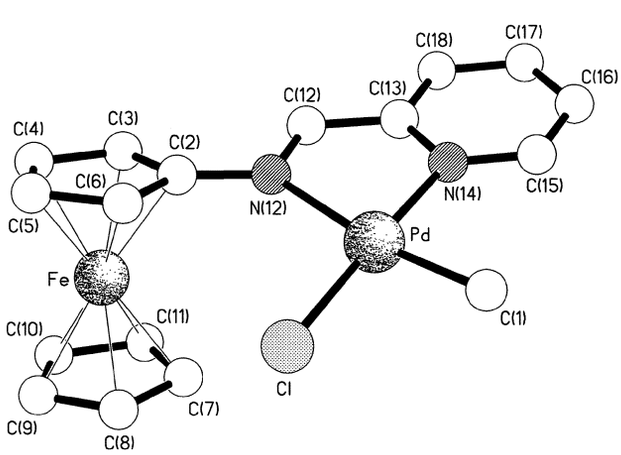

Fig. 3 One of the pair (A) of crystallographically independent molecules present in the structure of **6B**. The non-bonded Pd ··· Fe distances are 4.52 (A) and 4.64 Å (B).

Table 1 Selected bond lengths (Å) and angles (°) for **6B**

	Mol. A	Mol. B		Mol. A	Mol. B
Pd–Cl	2.306(2)	2.308(2)	Pd–C(1)	2.025(6)	2.018(7)
Pd–N(12)	2.206(5)	2.214(5)	Pd–N(14)	2.053(6)	2.057(5)
N(12)–C(12)	1.287(9)	1.282(8)			
Cl–Pd–C(1)	87.2(2)	87.4(3)	Cl–Pd–N(12)	101.4(2)	101.68(13)
Cl–Pd–N(14)	175.22(14)	179.0(2)	C(1)–Pd–N(12)	171.0(3)	170.7(3)
C(1)–Pd–N(14)	93.0(3)	91.8(3)	N(12)–Pd–N(14)	78.6(2)	79.1(2)

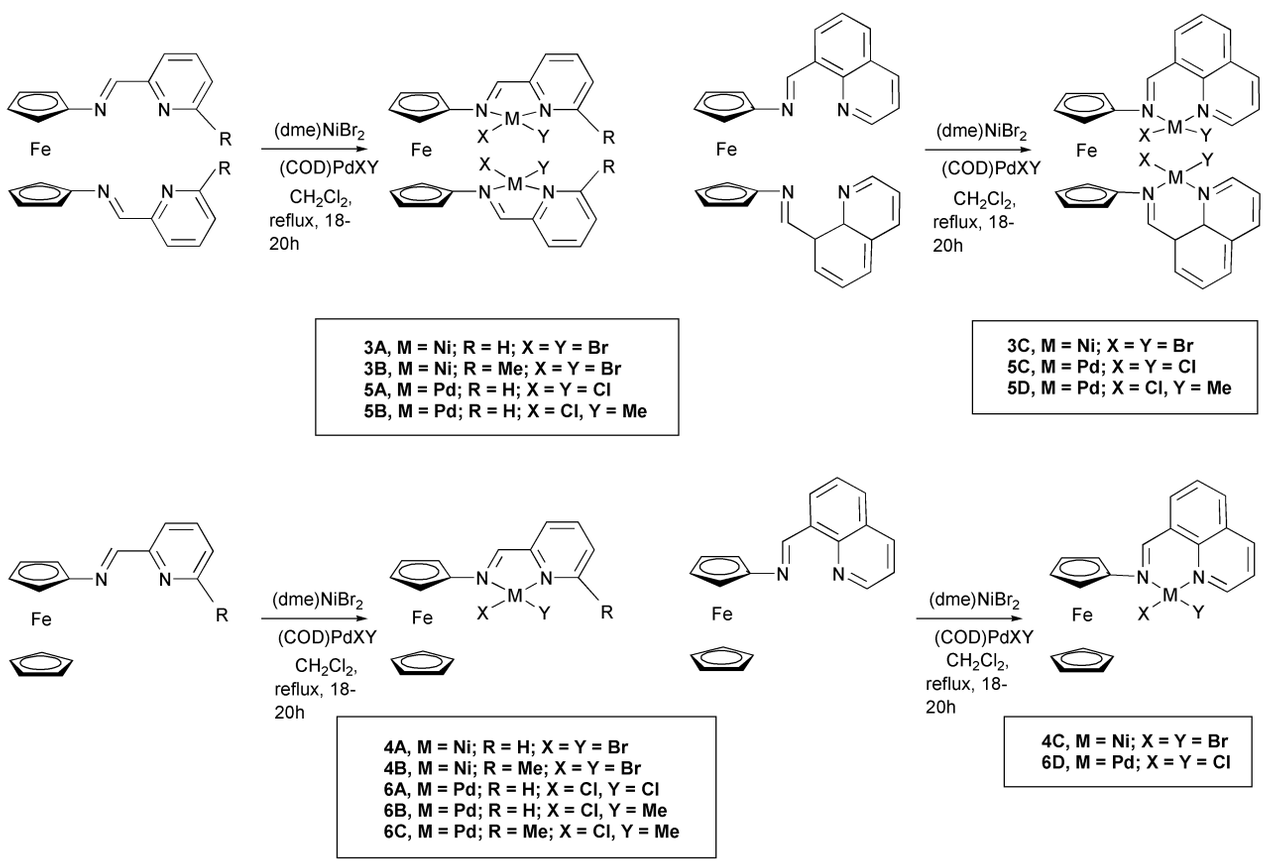

Scheme 2 Formation of complexes **3A**–**6D**.

rings are coplanar to within 0.07 Å but with the chloride deviating by only 0.01 Å from this plane. The resulting non-bonded Cl ··· Fe distances are 4.19 and 4.64 Å, respectively. It is noteworthy that in molecule A the pyridyl ring is more steeply inclined (by *ca*. 16°) to its adjacent C_5H_4 ring that it is in molecule B (by *ca*. 9°). There is a slightly greater degree of stagger (*ca*. 10°) of the cyclopentadienyl rings in both molecules than was observed in **1A** and **1C**, the maximum inter-ring tilt angle being *ca*. 4° (in molecule A). In both molecules the Pd–N distances differ with those *trans* to chlorine being significantly shorter than those *trans* to methyl (Table 1); the integrity of the C=N linkage is also retained [1.287(9) and 1.282(8) Å, respectively]. The dominant intermolecular packing feature is the formation, by molecules of type B, of continuous π–π stacks of C_i-related pairs of molecules (Fig. 4). There is also a weak intermolecular C–H ··· π interaction between independent molecules, the C(4)–H hydrogen of molecule B approaching the N(14) pyridyl ring of molecule A (H ··· π 2.70 Å, C–H ··· π 166°).

Chelation of both arms of ligand **2A** results in the pseudo C_2-symmetric structure for **5B** depicted in Fig. 5. The adoption of approximate C_2 symmetry by the complex, *cf*. C_s in the ligand, results in the imino bond and its associated pyridyl ring system in one arm being offset with respect to their counterparts in the other such that there are no longer any intramolecular π-π stacking interactions; the Pd(1) ··· Pd(2) separation is 3.77 Å. The inclination of the palladium coordination planes with respect to their associated cyclopentadienyl ring planes (*ca*. 19°) is such as to reduce the intramolecular Pd ··· Pd separation. For Pd(1) the pyridyl and chelate rings and metal coordination plane are coplanar to within 0.03 Å, whereas for Pd(2) the palladium atom and the chelate and pyridyl rings are planar to within 0.02 Å but with the chloride and methyl carbon atoms lying 0.10 and 0.20 Å, respectively, out of this plane. The cyclopentadienyl rings have a *ca*. 6° stagger and are inclined by *ca*. 3°. The geometry at each palladium centre is distorted square planar, the *cis* angles being in the ranges 78.9(2)–101.3(2) and 79.5(3)–100.1(2)° at Pd(1) and Pd(2), respectively, the most acute angles being associated with the bite of the *N*,*N*′ chelate ring. As was seen in **6B**, the Pd–N bonds *trans* to chlorine are significantly shorter than those *trans* to methyl; in both ligand arms the C=N double bond character has been retained (Table 2). There are no intermolecular packing interactions of note. There is some disorder in the structure with, in *ca*. 50% of the molecules, incomplete methylation of the Pd(2) centre having occurred, resulting in a mixture of $PdCl_2$ and PdClMe species distributed throughout the crystal; the overall effects on the rest of the structure are minimal, and are reflected only in the length of the Pd(2)–X [X = C(2), Cl(3)] bond.

It is interesting that the introduction of methyl substituents on the pyridyl rings *meta* to the imino unit results in the formation of a very different type of complex (**7A** and **7B**) on

Table 2 Selected bond lengths (Å) and angles (°) for **5B**

Pd(1)–Cl(1)	2.311(2)	Pd(2)–Cl(2)	2.303(3)
Pd(1)–C(1)	2.057(7)	Pd(2)–C(2)	2.058(2)
Pd(1)–N(13)	2.187(6)	Pd(2)–N(20)	2.127(6)
Pd(1)–N(15)	2.056(7)	Pd(2)–N(22)	2.052(8)
N(13)–C(13)	1.281(9)	N(20)–C(20)	1.274(11)
Cl(1)–Pd(1)–C(1)	87.3(2)	Cl(2)–Pd(2)–C(2)	85.3(9)
Cl(1)–Pd(1)–N(13)	101.3(2)	Cl(2)–Pd(2)–N(20)	100.1(2)
Cl(1)–Pd(1)–N(15)	179.3(2)	Cl(2)–Pd(2)–N(22)	176.8(2)
C(1)–Pd(1)–N(13)	171.4(3)	C(2)–Pd(2)–N(20)	173.8(9)
C(1)–Pd(1)–N(15)	92.5(3)	C(2)–Pd(2)–N(22)	95.3(9)
N(13)–Pd(1)–N(15)	78.9(2)	N(20)–Pd(2)–N(22)	79.5(3)

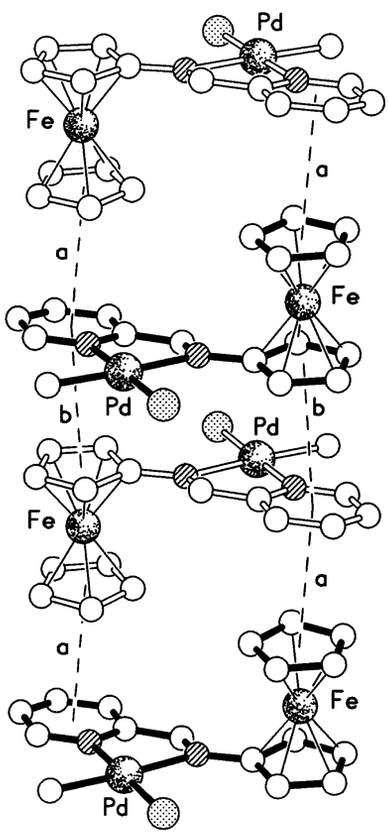

Fig. 4 Part of one of the π–π stacked chains of molecules (B) present in the structure of **6B**. The centroid ··· centroid separations are **a**) 3.46 and **b**) 3.47 Å.

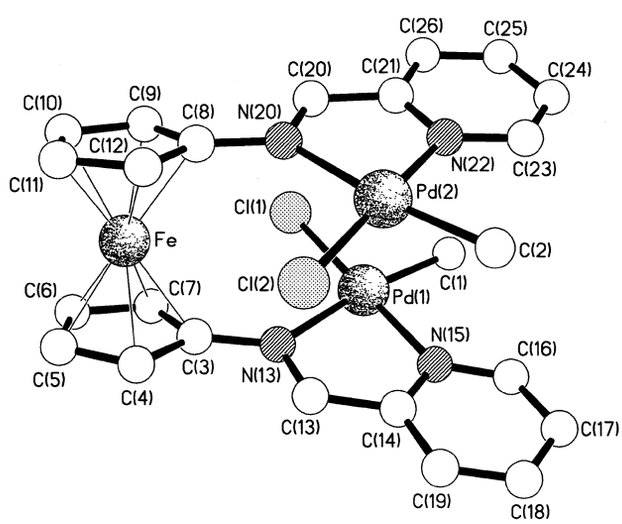

Fig. 5 The molecular structure of **5B**. The non-bonded Pd ··· Fe separations are 4.57 [Pd(1)] and 4.49 [Pd(2)] Å, respectively.

Table 3 Selected bond lengths (Å) and angles (°) for **7A**

Pd–Cl(1)	2.3012(14)	Pd–Cl(2)	2.3110(13)
Pd–N(13)	2.053(5)	Pd–N(21)	2.055(5)
N(11)–C(11)	1.262(7)	N(19)–C(19)	1.266(7)
Cl(1)–Pd–Cl(2)	177.39(6)	Cl(1)–Pd–N(13)	90.16(12)
Cl(1)–Pd–N(21)	88.32(12)	Cl(2)–Pd–N(13)	89.26(12)
Cl(2)–Pd–N(21)	92.19(12)	N(13)–Pd–N(21)	177.9(2)

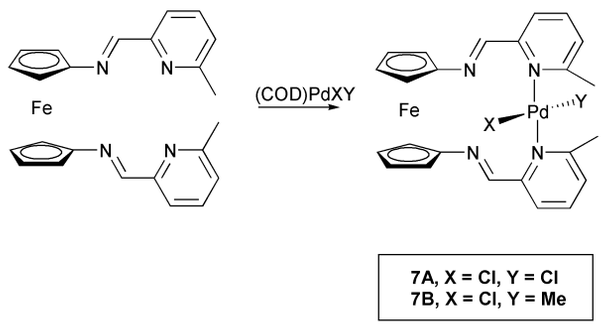

Scheme 3 Formation of complexes **7A** and **7B**.

reaction with (COD)PdCl(X) {X = Cl, Me} (Scheme 3). Perhaps surprisingly, only mono-palladium species were formed on reaction of the ligands with 1 *and* 2 molar equivalents of (COD)PdCl(X). The X-ray analysis of **7A** shows that instead of both iminopyridyl arms of the ligand chelating to separate metal centres as was observed in **5B**, here each ligand arm retains a *trans* relationship between the pyridyl and imino nitrogen atoms and a single palladium centre links the pyridyl nitrogen atoms of opposing arms (Fig. 6). The geometry at palladium is only slightly distorted square planar, the *cis* angles ranging between 88.3(1) and 92.2(1)° with the Pd–N distances (Table 3) being comparable to those to the pyridyl nitrogen atoms in **6B** and **5B**. The metal coordination plane (which is planar to within 0.03 Å) is oriented approximately orthogonally (*ca.* 79°) to its associated pyridyl ring systems which in turn are inclined by 30 and 24° [for the N(13)- and N(21)-containing rings, respectively] to their adjacent cyclopentadienyl ring planes. The palladium atom is displaced slightly out of its coordination plane away from the iron centre which is 5.50 Å distant; despite the apparently open nature of the metallacyclic ring, it is in fact self-filling. The C_5H_4 rings are staggered by *ca.* 7° with the N(11) ··· C_5-(centroid) and N(19) ··· C_5(centroid) vectors being staggered by *ca.* 82°. There are no noteworthy intermolecular packing interactions.

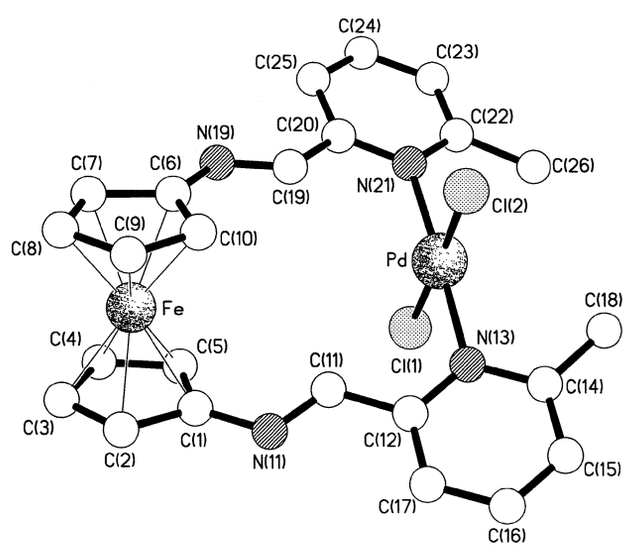

Fig. 6 The molecular structure of **7A**.

Table 4 Electrochemical data

	E_p^a/V	E_p^c/V	$E_{1/2}$/V	ΔE_p/V	E_p^c (2)/V
1A	0.567	0.479	0.523	0.088	
1B	0.540	0.450	0.495	0.09	
2A	0.553	0.457	0.505	0.096	
2B	0.546	0.456	0.501	0.09	0.185
2C	0.488	0.410	0.449	0.078	0.161
6A	0.668	0.592	0.630	0.076	
6D	0.665	0.575	0.62	0.09	

Electrochemistry. Cyclic voltammetry studies on a range of the ligands and complexes show that in each case quasi-reversible one electron transfers for the Fe^{II}–Fe^{III} redox couple of the ferrocenyl species are observed (Table 4, Fig. 7). There is little influence on the overall redox chemistry by the imino and/or pyridyl functionalities. The nature of substituent groups on the pyridyl rings does slightly influence the redox chemistries of the ligands, as reflected by the difference in redox potential between **1A** and **1B**. This influence on the redox potentials is less pronounced for **2A** and **2B**, probably due to the presence of one rather than two pyridyl groups.

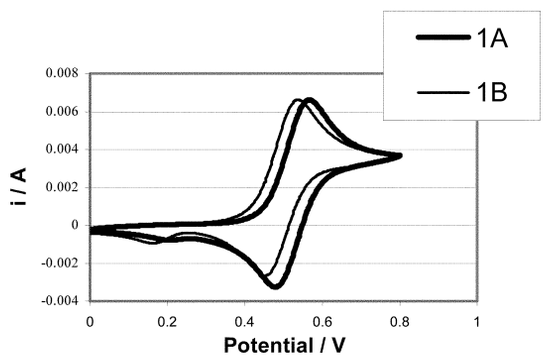

Fig. 7 Electrochemical data for **1A** and **1B**.

In the case of the ligands, a reduction is noted at *ca*. 0.5 V, which is consistent with the electrochemical reduction of the imine species to an amine group. This reduction is irreversible on the timescale of the electrochemical experiments. In addition, the chemical reduction can be easily carried out using standard reduction techniques (*i.e*. Zn/HCl or $LiAlH_4$). As is expected,[10,15] on coordination of a metal centre(s) to the ligands, the Fe^{II}/Fe^{III} oxidation shifts to higher positive potential *i.e.* oxidation becomes more difficult (Fig. 8). There are no other electron transfer processes observed in the potential window.

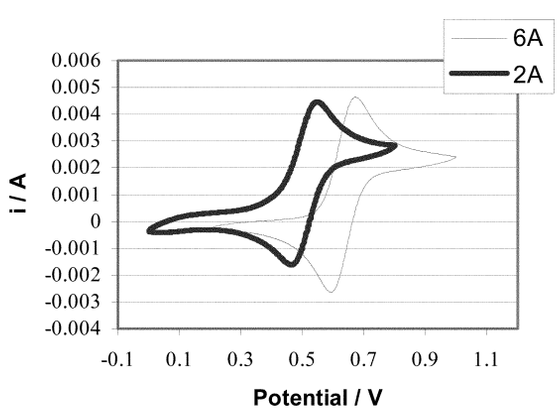

Fig. 8 Electrochemical data for **2A** and **6A**.

Polymerisation studies. Polymerisation reactions were performed by dissolving 10 μmol of pre-catalyst in toluene (100 ml) in a Schlenk tube under pressure of ethylene (1 bar) in the presence of 100 equivalents of methylaluminoxane (MAO) as co-catalyst. After 1 h, the reaction was terminated by removing the ethylene and exposing the flask to air, with the reaction mixture being worked up with 1 M HCl solution. In each case, there was no visible precipitation of polymer but the organic layer was analysed by gas chromatography in order to determine whether any oligomerisation had occurred (Table 5).

The palladium species were found to be inactive, but with the nickel-based complexes, although no high molecular weight polyethylene was formed, these pre-catalysts are highly selective for the formation of short chain oligomers and particularly, butenes with trace amounts of higher oligomers (C_6 and C_8), with **4A** particularly, showing an excellent TON. It is clear that β–H transfer is favoured over chain propagation thus leading to dimer formation, presumably due to lack of protection of the metal centre by the ferrocenyl units. In similar systems featuring bulky aryl groups instead of ferrocenyl,[14] steric protection of the metal centre is offered by *ortho*-substitution on the arylamine units and branched polymers are produced. The presence of a warm reaction mixture at the end of the catalytic run indicates that the nickel catalysts have a substantial lifetime and are capable of promoting the reaction over a prolonged period without significant decay, although further testing is needed to determine the profile of the catalyst lifetime. **8** (the chemically oxidised PF_6 salt of **4A**) was formed and also tested under the polymerisation conditions and it is interesting that in this case, the ferrocenium species gave no advantage over its neutral counterpart. We believe that the MAO used to activate the pre-catalyst is responsible for reducing the ferrocenium species back to its neutral ferrocenyl complex. Subsequent tests show that ferrocenium hexafluorophosphate is indeed reduced to ferrocene on addition of MAO.

Clearly, control of catalysis *via* redox-activity is still at a preliminary stage and this is the focus of on-going research.

Experimental

All preparations were carried out using standard Schlenk techniques.[16] All solvents were distilled over standard drying agents under nitrogen directly before use and deoxygenated. All reactions were carried out under an atmosphere of nitrogen. All NMR spectra were recorded on a Bruker AC250 instrument. Chemical shifts are reported in δ and referenced to residual proton impurity using $CDCl_3$ ($CHCl_3$ δ 7.26 ppm) or C_6D_6 (C_6D_5H δ 7.15 ppm). Mass spectra were recorded on a Micromass Autospec mass spectrometer with a 35 keV Cs^+ primary ion beam and a 3-nitrobenzyl alcohol matrix for FAB mass spectrometry. Microanalyses were carried out by Stephen Boyer at the University of North London. Cyclic voltammetric studies were carried out using tetra(*tert*-butyl)ammonium hexafluorophosphate as the electrolyte and dichloromethane as the solvent. A standard calomel electrode was used as the reference electrode, along with platinum working and auxiliary electrodes. The scan rate was 100 mV s^{-1}.

Ferrocenylamine,[6] 1,1′-diaminoferrocene,[7] 6-methyl-2-pyridinealdehyde,[17] and 8-quinoline carbaldehyde[18] were formed *via* modified literature procedures and all other starting materials were obtained from commercial sources.

Synthesis of 1A

To a solution of 1,1′-diaminoferrocene (0.21 g, 1 mmol) in dichloromethane (50 ml) was added pyridine-2-carbaldehyde (0.19 ml, 2 mmol). The solution was stirred for 5 h and the solvent removed *in vacuo*. The resulting burgundy coloured solid was washed with pentane (2 × 20 ml) and dried under vacuum to yield **1A** (0.3 g, 76%). Elemental analysis: found: C 66.9, H 4.7, N 14.1; requires: C 67.0, H 4.6, N 14.2%. ^{1}H NMR ($CDCl_3$): δ 4.28 (4H, t, C_5H_4-Cp), 4.66 (4H, t, C_5H_4-Cp), 7.14 (2H, m, C_5H_4-py), 7.44 (2H, m, C_5H_4-py), 7.80 (2H, m,

Table 5 Products and turnover numbers (TON) from polymerisation tests

Compound	Products	TON (no. of moles substrate/per mole of catalyst) ($\times 10^3$)
3A	Dimer (butenes)	4.42
3B	Dimer	3.36
3C	Dimer + traces of trimer (hexanes)	1.64
4A	Dimer + traces of higher oligomers	19.14
4B	Dimer	11.82
4C	Dimer and trimer	2.57
8	Dimer + traces of trimer	16.43

C_5H_4-py) 8.44 (2H, m, C_5H_4-py), 8.47 (2H, s, N=CH). ^{13}C-{^{1}H} NMR ($CDCl_3$): δ 64.8, 69.4, 104.0, 120.9, 123.9, 136.2, 149.3, 154.9, 158.6. FAB$^+$ MS: *m*/*z* 394 ([M]$^+$).

Synthesis of 1B

An analogous procedure to that described for **1A** was followed using 1,1′-diaminoferrocene (0.21 g, 1 mmol) and 6-methylpyridine-2-carbaldehyde (0.24 g, 2 mmol). Yield: 0.35 g, 83%. Elemental analysis: found: C 68.4, H 5.4, N 13.2; requires: C 68.2, H 5.2, N 13.2%. ^{1}H NMR ($CDCl_3$): δ 2.52 (6H, s, CH_3), 4.32 (4H, t, C_5H_4-Cp), 4.69 (4H, t, C_5H_4-Cp), 7.05 (2H, d, C_5H_3) 7.38 (2H, t, C_5H_3), 7,71 (2H, d, C_5H_3), 8.48 (2H, s, N=CH). ^{13}C-{^{1}H} NMR ($CDCl_3$): δ 24.2, 64.8, 69.3, 104.0, 117.9, 123.5, 136.3, 154.4, 157.7, 158.9. FAB$^+$ MS: *m*/*z* 422 ([M]$^+$).

Synthesis of 1C

An analogous procedure to that described for **1A** was followed using 1,1′-diaminoferrocene (0.21 g, 1 mmol) and quinoline–9-carbaldehyde (0.31 g, 2 mmol). Yield: 0.42 g, 85%. Elemental analysis: found: C 72.8, H 4.5, N 11.2; requires: C 72.9, H 4.4, N 11.3%. ^{1}H NMR ($CDCl_3$): δ 4.30 (4H, t, C_5H_4-Cp), 4.80 (4H, t, C_5H_4-Cp), 7.16 (4H, m, C_9H_6), 7.52 (2H, m, C_9H_6), 7.87 (2H, m, C_9H_6), 8.19 (2H, m, C_9H_6), 8.66 (2H, m, C_9H_6), 9.72 (2H, s, CH=N). ^{13}C-{^{1}H} NMR ($CDCl_3$): δ 64.8, 68.7, 105.8, 120.8, 126.1, 126.6, 127.7, 129.3, 133.1, 135.8, 145.9, 149.4, 155.5. FAB$^+$ MS: *m*/*z* 494 ([M]$^+$).

Synthesis of 2A

To a solution of ferrocenylamine (0.2 g, 1 mmol) in dichloromethane (40 ml) was added pyridine-2-carbaldehyde (0.1 ml, 1 mmol). The solution was stirred at 40 °C for 3 h. The solvent was removed *in vacuo*, and the resulting oily, burgundy solid extracted into hexane and filtered through a short pad of silica. Crystals of **2A** were grown from slow evaporation of the hexane solution. Yield: 0.15 g, 52%. Elemental analysis: found: C 66.3, H 4.8, N 9.6; requires: C 66.2, H 4.39, N 9.7%. ^{1}H NMR ($CDCl_3$): δ 4.19 (5H, s, C_5H_4-Cp), 4.32 (2H, t, C_5H_4-Cp), 4.67 (2H, t, C_5H_4-Cp) 7.34 (1H, t, C_5H_4-py), 7.76 (1H, t, C_5H_4-py), 8.11 (1H, t, C_5H_4-py), 8.65 (1H, t, C_9H_6), 8.75 (1H, s, CH=N). ^{13}C-{^{1}H} NMR ($CDCl_3$): δ 63.54, 67.79, 69.76, 115.35, 121.13, 124.34, 136.62, 149.61, 157.99. CI MS: *m*/*z* 290 ([M]$^+$)

Synthesis of 2B

An analogous procedure to that described for **2A** was employed using ferrocenylamine (0.2 g, 1 mmol) and 6-methylpyridine-2-carbaldehyde (0.12 g, 1 mmol). Yield: 0.12 g, 39%. Elemental analysis: found: C 67.0, H 5.4, N 9.2; requires: C 67.1, H 5.3, N 9.2%. ^{1}H NMR ($CDCl_3$): δ 2.59 (3H, s, Me), 4.17 (5H, s, C_5H_4-Cp), 4.28 (2H, t, C_5H_4-Cp), 4.65 (2H, t, C_5H_4-Cp) 7.22 (1H, d, C_5H_3), 7.65 (1H, m, C_5H_3), 7.96 (1H, m, C_5H_3), 8.69 (1H, s, CH=N). ^{13}C-{^{1}H} NMR ($CDCl_3$): δ 24.38, 63.56, 67.86, 69.73, 118.03, 124.03, 136.83, 154.68, 158.34. CI MS: *m*/*z* 304 ([M]$^+$)

Synthesis of 2C

An analogous procedure to that described for **2A** was employed using ferrocenylamine (0.2 g, 1 mmol) and quinoline-9-carbaldehyde (0.31 g, 2 mmol). Yield: 0.14 g, 41%. Elemental analysis: found: C 70.6, H 4.8, N 8.1; requires: C 70.6, H 4.7, N 8.2%. ^{1}H NMR ($CDCl_3$): δ 4.21 (5H, s, Cp), 4.30 (2H, t, C_5H_4-Cp), 4.74 (2H, t, C_5H_4-Cp) 7.45 (1H, m, C_9H_6), 7.63 (1H, m, C_9H_6), 7.92 (1H, m, C_9H_6), 8.19 (1H, m, C_9H_6), 8.56 (1H, m, C_9H_6) 8.97 (1H, m, C_9H_6), 10.02 (1H, s, CH=N). ^{13}C-{^{1}H} NMR ($CDCl_3$): δ 63.44, 67.38, 69.60, 121.34, 126.66, 126.97, 130.06, 136.25, 149.99, 155.64. CI MS: *m*/*z* 340 ([M]$^+$)

Synthesis of 3A

To a suspension of $NiBr_2$·dme (0.2 g, 0.66 mmol) in dichloromethane (30 ml) was added a solution of **1A** (0.15 g, 0.37 mmol) also in dichloromethane (25 ml). The mixture was heated at reflux for 19 h, during which time an indigo coloured precipitate had formed. The reaction mixture was filtered and the resulting blue solid washed with diethyl ether (2 × 20 ml) and dried *in vacuo* to yield **3A** (0.14 g, 52%). Elemental analysis: found: C 31.7, H 2.3, N 6.9; requires: C 31.8, H 2.2, N 6.7%. FAB$^+$ MS: *m*/*z* 750 ([M − Br]$^+$), 671 ([M − 2Br]$^+$).

Synthesis of 3B

An analogous procedure to that used for **3A** was employed using $NiBr_2$·dme (0.2 g, 0.66 mmol), and **1B** (0.15 g, 0.36 mmol). Yield: 0.16 g, 51%. Elemental analysis: found: C 33.6, H 2.6, N 6.6; requires: C 33.5, H 2.6, N 6.5%. FAB$^+$ MS: *m*/*z* 780 ([M − Br]$^+$).

Synthesis of 3C

An analogous procedure to that used for **3A** was employed using $NiBr_2$·dme (0.2 g, 0.66 mmol), and **1C** (0.18 g, 0.36 mmol). Yield: 0.18 g, 54%. Elemental analysis: found: C 38.5, H 2.2, N 5.9; requires: C 38.7, H 2.4, N 6.0%. FAB$^+$ MS: *m*/*z* 852 ([M − Br]$^+$).

Synthesis of 4A

An analogous procedure to that used for **3A** was employed using **2A** (0.14 g, 0.5 mmol) and $NiBr_2$·dme (0.14 g 0.45 mmol). Yield: 0.16 g, 63%. Elemental analysis: found: C 38.0, H 2.9, N 5.3; requires: C 37.8. H 2.8, N 5.5%. FAB$^+$ MS: *m*/*z* 508 ([M]$^+$), 429 ([M − Br]$^+$).

Synthesis of 4B

An analogous procedure to that used for **3A** was employed using **2B** (0.15 g, 0.5 mmol) and $NiBr_2$·dme (0.15 g, 0.45 mmol). Yield: 0.14 g, 54%. Elemental analysis: found: C 39.2, H 3.2, N 5.0; requires: C 39.1, H 3.1, N 5.4%. FAB$^+$ MS: *m*/*z* 522 ([M]$^+$), 443 ([M–Br]$^+$).

Synthesis of 4C

An analogous procedure to that used for **3A** was employed using **2C** (0.17 g, 0.5 mmol) and $NiBr_2$.dme (0.15 g, 0.45 mmol). Yield: 0.18 g, 65%. Elemental analysis: found: C 42.0, H 2.8, N 4.9; requires: C 42.0, H 2.9, N 5.0%. FAB$^+$ MS: *m*/*z* 479 ([M–Br]$^+$).

Synthesis of 5A

A solution of **1A** (0.14 g, 0.34 mmol) in dichloromethane (30 ml) was added to a solution of $(COD)PdCl_2$ (0.18 g, 0.63 mmol) also in dichloromethane (20 ml) and the resulting burgundy coloured solution stirred for 18 h, during which time a blue coloured precipitate formed. The reaction mixture was filtered and the remaining blue solid washed with dichloromethane (2 × 20 ml) and dried under vacuum to yield **5A** (0.19 g, 62%). Elemental analysis: found: C 35.3, H 2.4, N 7.6; requires: C 35.2, H 2.4, N 7.5%. ^{1}H NMR ($CDCl_3$): δ 4.48 (4H, t, C_5H_4-Cp), 5.58 (4H, m, C_5H_4-Cp), 7.56 (2H, m, C_5H_4-py), 7.87 (2H, m, C_5H_4-py), 8.05 (2H, m, C_5H_4-py), 8.41 (2H, s, N=CH), 8.97 (2H, m, C_5H_4-py). FAB^+ MS: *m*/*z* 748 ($[M]^+$), 712 ($[M - Cl]^+$).

Synthesis of 5B

A solution of **1A** (0.14 g, 0.34 mmol) in dichloromethane (30 ml) was added to a solution of (COD)Pd(Me)Cl (0.16 g, 0.61 mmol) also in dichloromethane (20 ml) and the resulting burgundy coloured solution stirred for 18 h, during which time a dark burgundy coloured precipitate formed. The reaction mixture was filtered and the resulting solid washed with dichloromethane (2 × 20 ml) and dried under vacuum to yield **5B** (0.19 g, 62%). Elemental analysis: found: C 40.9, H 3.4, N 8.0; requires: C 40.7, H 3.4, N 7.9%. ^{1}H NMR ($CDCl_3$): δ 0.51 (6H, s, Pd–Me) 4.41 (4H, t, C_5H_4-Cp), 5.80 (4H, m, C_5H_4-Cp), 7.38 (2H, m, C_5H_4-py), 7.82 (2H, m, C_5H_4-py), 7.92 (2H, m, C_5H_4-py), 8.89 (2H, s, N=CH). FAB^+ MS: *m*/*z* 708 ($[M]^+$).

Synthesis of 5C

An analogous procedure used for the synthesis of **5A** was employed using **1C** (0.24 g, 0.5 mmol) and $(COD)PdCl_2$ (0.28 g, 1 mmol) to yield mauve coloured solid **5C** (0.32 g, 75%). Elemental analysis: found: C 42.6, H 2.6, N 6.6; requires: C 42.4, H 2.6, N 6.6%. FAB^+ MS: *m*/*z* 850 ($[M]^+$).

Synthesis of 5D

An analogous procedure to that employed for **5B** was used, using **1C** (0.12 g, 0.25 mmol) and (COD)Pd(Me)Cl (0.12 g, 0.46 mmol) to yield the mauve coloured solid **5D** (0.17 g, 84%). Elemental analysis: found: C 47.2, H 3.5, N 7.1; requires: C 47.5, H 3.5, N 6.9%. FAB^+ MS: *m*/*z* 808 ($[M]^+$).

Synthesis of 6A

A solution of **2A** (0.84 g, 2.04 mmol) in dichloromethane (30 ml) was added to a solution of $(COD)PdCl_2$ (1.00 g, 3.53 mmol) also in dichloromethane (20 ml) and the resulting burgundy coloured solution stirred for 18 h, during which time a blue–purple coloured precipitate formed. The reaction mixture was filtered and the resulting blue coloured solid washed with dichloromethane (2 × 20 ml) and dried *in vacuo* to yield **6A** (1.04 g, 52%). Elemental analysis: found: C 41.0, H 3.1, N 5.9; requires: C 41.1, H 3.0, N 6.0%. ^{1}H NMR (d^6-DMSO): δ 4.39 (5H, s, C_5H_5), 4.45 (2H, t, C_5H_4-Cp), 5.06 (2H, t, C_5H_4-Cp), 7.87 (1H, t, Ar-H), 8.25 (1H, d, Ar-H), 8.34 (1H, t, Ar-H), 9.02 (1H, d, py-H), 9.13 (1H, s, Ar-H). FAB^+ MS: *m*/*z* 461 ($[M]^+$).

Synthesis of 6B

A solution of **2A** (0.12 g, 0.4 mmol) in dichloromethane (30 ml) was added to a solution of (COD)Pd(Me)Cl (0.1 g, 0.38 mmol) also in dichloromethane (20 ml) and the resulting burgundy coloured solution stirred for 18 h, during which time a blue–purple coloured precipitate formed. The reaction mixture was filtered and the resulting blue coloured solid washed with dichloromethane (2 × 20 ml) and dried *in vacuo* to yield **6B** (0.1 g, 52%). Elemental analysis for **6B**·$0.5CH_2Cl_2$: found: C 40.8, H 3.70, N 5.65; requires: C 40.0, H 3.43, N 5.33%. ^{1}H NMR (d^6-acetone): δ 1.10 (3H, s, CH_3), 4.37 (5H, s, C_5H_5), 4.45 (2H, t, β-C_5H_4-Cp), 5.49 (2H, t, α-C_5H_4-Cp), 7.80 (1H, t, Ar-H), 8.01 (1H, d, Ar-H), 8.25 (2H, m, Ar-H), 8.67 (1H, d, py-H), 8.98 (1H, s, Ar-H). FAB^+ MS: *m*/*z* 448 ($[M]^+$).

Synthesis of 6C

An analogous procedure used for the synthesis of **6B** was employed using **2B** (0.14 g, 0.46 mmol) and (COD)Pd(Me)Cl (0.12 g, 0.45 mmol) to yield mauve coloured solid **6C** (0.09 g, 43%). Elemental analysis: found: C 46.7, H 4.1, N 6.0; requires: C 46.9, H 4.2, N 6.1%. ^{1}H NMR (d^6-acetone): δ 0.94 (3H, s, Pd–CH_3), 2.57 (3H, s, py–CH_3), 4.38 (5H, s, C_5H_5), 4.45 (2H, t, C_5H_4-Cp), 5.49 (2H, t, C_5H_4-Cp), 7.80 (1H, t, Ar-H), 8.01 (1H, d, Ar-H), 8.25 (1H, t, Ar-H), 8.67 (1H, d, py-H), 8.98 (1H, s, Ar-H). FAB^+ MS: *m*/*z* 409 ($[\mathbf{6C} - Pd]^+$).

Synthesis of 6D

An analogous procedure used for the synthesis of **6A** was employed using **2C** (0.2 g, 0.58 mmol) and $(COD)PdCl_2$ (0.25 g, 0.87 mmol) to yield mauve coloured solid **6D** (0.13 g, 43%). Elemental analysis: found: C 44.6, H 3.0, N 4.5; requires: C 44.4, H 3.1, N 5.4%. ^{1}H NMR (d^6-acetone): δ 4.21 (5H, s, C_5H_5), 4.37 (2H, t, C_5H_4-Cp), 5.29 (2H, t, C_5H_4-Cp), 7.85 (1H, m, Ar-H), 8.00 (1H, m, Ar-H), 8.50 (1H, d, Ar-H), 8.67 (1H, d, Ar-H), 8.85 (1H, d, Ar-H), 9.15 (1H, s, C=NH), 9.67 (1H, d, Ar-H). FAB^+ MS: *m*/*z* 518 ($[M]^+$).

Synthesis of 7A

A mixture of **1B** (0.21 g, 0.5 mmol) and $(COD)PdCl_2$ (0.14 g, 0.5 mmol) were charged to a Schlenk vessel and dichloromethane (50 ml) added. The resulting burgundy coloured solution was heated to 40 °C for 14 h, by which time the colour had changed to purple. The volatiles were removed *in vacuo* and the resulting purple solid recrystallised from dichloromethane–pentane (30 : 70) to yield purple crystalline **7A** (0.24 g, 80%). Elemental analysis: found: C 48.0, H 3.6, N 9.5; requires: C 48.1, H 3.7, N 9.3%. ^{1}H NMR ($CDCl_3$): δ 3.65 (6H, s, Me) 4.55 (4H, t, C_5H_4-Cp), 4.67 (4H, t, C_5H_4-Cp), 7.36 (2H, m, C_5H_3), 7.70 (2H, m, C_5H_3), 7.93 (2H, m, C_5H_3), 11.14 (2H, s, N=CH). ^{13}C-{^{1}H} NMR ($CDCl_3$): δ 27.4, 68.3, 69.1, 103.7, 121.7, 126.5, 138.9, 155.6, 158.4, 161.1. FAB^+ MS: *m*/*z* 563 ($[M - Cl]^+$)

Synthesis of 7B

An analogous procedure to that employed for **7A** was utilised using **1B** (0.21 g, 0.5 mmol) and (COD)Pd(Me)Cl (0.13 g, 0.5 mmol). This yielded purple crystalline **7B** (0.2 g, 69%). Elemental analysis: found: C 51.7, H 4.4, N 9.5; requires: C 51.8, H 4.3, N 9.7%. ^{1}H NMR ($CDCl_3$): δ 0.33 (3H, s, Pd–Me) 3.42 (6H, s, Me), 4.50 (6H, m, C_5H_4), 4.59 (2H, m, C_5H_4), 7.36 (2H, m, C_5H_3), 7.73 (2H, m, C_5H_3), 7.94 (2H, m, C_5H_3), 10.84 (2H, s, N=CH). FAB^+ MS: *m*/*z* 543 ($[M - Cl]^+$)

Synthesis of 8

In a Schlenk vessel a suspension of **4A** (0.06 g, 0.12 mmol) was stirred with ferrocenium hexafluorophosphate (0.04 g, 0.12 mmol) in acetonitrile for 3 h. The volatiles were removed *in vacuo*. The resulting solid was heated to 50 °C for 3 h, after which ferrocene crystals began to sublime. The product was washed with hexane and dried to yield **8** (0.05 g, 65%). Elemental analysis: found: C, 29.6, H 2.4, N 4.3; requires: C 29.4, H 2.2, N 4.3%.

Ethylene polymerisation of 3 and 4

A solution of MAO in toluene (0.63 ml, 1 mmol, 100 equivalents) was added *via* a syringe to a stirred suspension of

Table 6 Crystal data, data collection and refinement parameters for compounds **1A**, **1C**, **5B**, **6B**, **7A**[a]

Data	**1A**	**1C**	**6B**	**5B**	**7A**
Formula	$C_{22}H_{18}N_4Fe$	$C_{30}H_{22}N_4Fe$	$C_{17}H_{17}N_2ClFePd$	$(C_{24}H_{24}N_4Cl_2FePd_2)_{0.5}$ $(C_{23}H_{21}N_4Cl_3FePd_2)_{0.5}$	$C_{24}H_{22}N_4Cl_2FePd$
Solvent	–	$0.5CH_2Cl_2{\cdot}0.5H_2O$	$0.5CH_2Cl_2$	$CHCl_3$	CH_2Cl_2
Formula weight	394.3	545.8	489.5	837.6	684.5
Colour, habit	Deep red blocks	Deep red blocks	Very dark orange platy prisms	Deep orange/red prisms	Deep red prisms
Crystal size/mm	0.67 × 0.57 × 0.40	0.50 × 0.40 × 0.20	0.60 × 0.43 × 0.40	0.40 × 0.27 × 0.10	0.50 × 0.47 × 0.40
Temperature/K	293	293	183	293	293
Crystal system	Orthorhombic	Triclinic	Monoclinic	Monoclinic	Monoclinic
Space group	*Pbca* (no. 61)	$P\bar{1}$ (no. 2)	$P2_1/c$ (no. 14)	$P2_1/c$ (no. 14)	$P2_1/c$ (no. 14)
a/Å	16.418(1)	10.980(2)	10.063(1)	18.852(1)	13.983(1)
b/Å	10.474(1)	13.481(1)	22.804(3)	7.661(1)	8.892(1)
c/Å	20.919(1)	18.574(2)	15.739(2)	19.625(1)	21.991(1)
α/°	–	100.24(1)	–	–	–
β/°	–	96.55(1)	97.26(1)	93.84(1)	107.04(1)
γ/°	–	108.48(1)	–	–	–
V/Å^3	3597.2(6)	2522.9(5)	3582.6(8)	2828.2(5)	2614.1(3)
Z	8	4[b]	8[b]	4	4
D_c/g cm^{-3}	1.456	1.437	1.815	1.967	1.739
Radiation used	Mo-Kα	Mo-Kα	Mo-Kα	Cu-Kα	Mo-Kα
μ/mm^{-1}	0.852	0.734	2.11	19.18	1.67
θ range/°	2.0–25.0	1.8–25.0	1.8–25.0	2.4–60.0	1.9–25.0
No. of unique reflections					
Measured	3148	8738	6256	4206	4601
Observed, $\lvert F_o\rvert > 4\sigma(\lvert F_o\rvert)$	2175	5516	4437	3291	3494
Absorption correction	–	–	Empirical	Empirical	Ellipsoidal
Max., min. transmission	–	–	0.69, 0.23	0.70, 0.24	0.51, 0.44
No. of variables	244	689	426	373	316
*R*1 wR_2[c]	0.041, 0.083	0.060, 0.141	0.044, 0.085	0.049, 0.113	0.041, 0.093

[a] Details in common: graphite monochromated radiation, refinement based on F^2. [b] There are two crystallographically independent molecules in the asymmetric unit. [c] $R_1 = \Sigma||F_o| - |F_c||/\Sigma|F_o|$; $wR_2 = \{\Sigma[w(F_o^2 - F_c^2)^2]/\Sigma[w(F_o^2)^2]\}^{1/2}$; $w^{-1} = \sigma^2(F_o^2) + (aP)^2 + bP$.

compound (0.01 mmol Ni) in toluene (100 ml). In all cases a blue–green solution was formed. The catalyst system was degassed under reduced pressure and back-filled with an atmosphere of ethylene. Fuming was observed. During the run time the solution was left open to a supply of ethylene at one atmosphere and stirred vigorously. The polymerisation was terminated by the addition of dilute HCl (100 ml) and stirring for 10 min. A sample of the toluene layer was removed, passed through a wad of alumina and used for GC analysis.

GC analysis was carried out on an Agilent 6890A GC with a HP-5 column (30 mm × 0.32 mm, film thickness 0.25 mm). The injected volume is 1 ml; The carrier gas is helium, 1.2 ml min^{-1}; Inlet 325 °C; FID detector 325 °C; Temp. program: isothermal for 5 min at 50 °C, followed by a 10 °C min^{-1} ramp to 300 °C and 10 min isothermal at 300 °C. Post-run: 7 min at 325 °C (to clean the column). The products were measured relative to a heptane internal standard.

X-Ray crystallography

Table 6 provides a summary of the crystallographic data for compounds **1A**, **1C**, **5B**, **6B** and **7A**. Data were collected on Siemens P4/PC diffractometers using ω-scans. The structures were solved by direct methods and they were refined based on F^2 using the SHELXTL program system.[19] The structure of **5B** is disordered at the Pd(2) centre, there being a *ca*. 50 : 50 mixture of $PdCl_2$ and PdClMe species distributed throughout the crystal

CCDC reference numbers 196185–196189.

See http://www.rsc.org/suppdata/dt/b2/b210463f/ for crystallographic data in CIF or other electronic format.

Acknowledgements

Johnson Matthey plc is thanked for the loan of precious metal salts.

References

1 A. M. Allgeier and C. A. Mirkin, *Angew. Chem., Int. Ed.*, 1998, **37**, 894.
2 I. M. Lorkovic, R. R. Duff, Jr. and M. S. Wrighton, *J. Am. Chem. Soc.*, 1995, **117**, 3617.
3 For a detailed literature review, see: A. Togni and T. Hayashi (Editors), *Ferrocenes: Homogeneous Catalysis – Organic Synthesis – Materials Science*, VCH, Weinheim, Germany, 1995; A. Togni and R. L. Halterman (Editors), *Metallocenes*, Wiley-VCH, Weinheim, Germany, 1998.
4 For a comprehensive overview of ferrocene and other metallocene chemistry, see: N. J. Long, in *Metallocenes: An Introduction to Sandwich Complexes*, Blackwell Science, Oxford, 1998.
5 K.-P. Stahl, G. Boche and W. Massa, *J. Organomet. Chem.*, 1984, **277**, 113; H. Plenio and D. Burth, *Organometallics*, 1996, **15**, 4054; H. Plenio and D. Burth, *Angew. Chem., Int. Ed. Engl.*, 1995, **34**, 800; B. Neumann, U. Siemeling, H.-G. Stammler, U. Vorfeld, J. G. P. Delis, P. W. N. M. van Leeuwen, K. Vrieze, J. Fraanje, K. Goubitz, F. Fabrizi de Biani and P. Zanello, *J. Chem. Soc., Dalton Trans.*, 1997, 4705; M. Herberhold, M. Ellinger and W. Kremnitz, *J. Organomet. Chem.*, 1983, **241**, 227; J. D. Carr, S. J. Coles, M. B. Hursthouse, M. E. Light, E. L. Munro, J. H. R. Tucker and J. Westwood, *Organometallics*, 2000, **19**, 3312; J. D. Carr, S. J. Coles, M. B. Hursthouse and J. H. R. Tucker, *J. Organomet. Chem.*, 2001, **637–639**, 304; B. Wrackmeyer, H. E. Maisel and M. Herberhold, *J. Organomet. Chem.*, 2001, **637–639**, 727; U. Siemeling, U. Vorfield, B. Neumann, H. -G. Stammler, P. Zanello and F. Fabrizi de Biani, *Eur. J. Inorg. Chem.*, 1999, **38**, 1; K. Kavallieratos, S. Hwang and R. H. Crabtree, *Inorg. Chem.*, 1999, **38**, 5184; I. R. Butler, *J. Organomet. Chem.*, 1997, **552**, 53; S. Bradley, P. C. McGowan, K. A. Oughton, M. Thornton-Pett and M. E. Walsh, *Chem. Commun.*, 1999, 77; S. Bradley, K. D. Camm, X. Liu, P. C. McGowan, R. Mumtaz, K. A. Oughton, T. J. Podesta and M. Thornton-Pett, *Inorg. Chem.*, 2002, **41**, 715.
6 D. van Leusen and B. Hessen, *Organometallics*, 2001, **20**, 224.
7 A. Shafir, M. P. Power, G. D. Whitener and J. Arnold, *Organometallics*, 2000, **19**, 3978; A. Shafir, D. Fiedler and J. Arnold, *J. Chem. Soc., Dalton Trans.*, 2002, 555.
8 A. Shafir, M. P. Power, G. D. Whitener and J. Arnold, *Organometallics*, 2001, **20**, 1365.
9 U. Siemeling, O. Kuhnert, B. Neumann, A. Stammler, H.-G. Stammler, B. Bildstein, M. Malaun and P. Zanello, *Eur. J. Inorg. Chem.*, 2001, 913.

10 V. C. Gibson, N. J. Long, E. L. Marshall, P. J. Oxford, A. J. P. White and D. J. Williams, *J. Chem. Soc., Dalton Trans.*, 2001, 1162.
11 M. Herberhold, *Angew. Chem., Int. Ed.*, 2002, **41**, 956.
12 G. J. P. Britovsek, V. C. Gibson and D. F. Wass, *Angew. Chem., Int. Ed.*, 1999, **38**, 428.
13 S. D. Ittel, L. K. Johnson and M. Brookhart, *Chem. Rev.*, 2000, **100**, 1169.
14 P.-L. Bres, V. C. Gibson, L. D. F. Mabille, W. Reed, D. F. Wass and R. H. Weatherhead (BP Chemicals), *World Pat*., WO 9849208 (1998); T. V. Laine, K. Lappalainen, J. Liimatta, E. Aitolu, B. Lofgren and M. Leskela, *Macromol. Rapid Commun.*, 1999, **20**, 487; T. V. Laine, M. Klinga and M. Leskeal, *Eur. J. Inorg. Chem.*, 1999, 959; T. V. Laine, U. Piiranen, K. Lappalainen, M. Klinga, E. Aitola and M. Leskela, *J. Organomet. Chem.*, 2000, **606**, 112; S. P. Meneghetti, P. J. Lutz and J. Kress, *Organometallics*, 1999, **18**, 2734; A. Koppl and H. G. Alt, *J. Mol. Catal. A: Chem.*, 2000, **154**, 45; R. Kempe, *Angew. Chem., Int. Ed.*, 2000, **39**, 468; T. Schareina, G. Hillebrand, H. Fuhrmann and R. Kempe, *Eur. J. Inorg. Chem.*, 2001, 2421.
15 V. C. Gibson, N. J. Long, A. J.P. White, C. K. Williams, D. J. Williams, M. Fontani and P. Zanello, *J. Chem. Soc., Dalton Trans.*, 2002, 3280.
16 R. J. Errington, *Advanced Practical Inorganic and Metalorganic Chemistry*, Blackie, London, 1997.
17 S. Kasuga and T. Taguchi, *Chem. Pharm. Bull.*, 1965, **13**, 233.
18 M. Seyhan and W. C. Fernelius, *J. Org. Chem.*, 1957, **22**, 217.
19 SHELXTL PC version 5.03, Siemens Analytical X-Ray Instruments, Inc., Madison, WI, 1994; SHELXTL PC version 5.1, Bruker AXS, Madison, WI, 1997.